Invertible Subset LDPC Code For PAPR Reduction In OFDM Systems With Low Complexity

Daiming Qu, Li Li and Tao Jiang

Abstract—**In this paper, we introduce a new family of low-density parity-check (LDPC) codes, called as invertible subset LDPC (IS-LDPC) code, for peak-to-average power ratio (PAPR) reduction in OFDM systems with low complexity. An IS-LDPC code has a number of disjoint invertible subsets, and each invertible subset can be independently inverted to generate other valid codewords of the LDPC code. To construct IS-LDPC codes with good error-correcting performance, we propose a modified progressive edge-growth construction algorithm and verify its effectiveness by analyzing the constructed Tanner graphs. Both theoretical analysis and numerical results show that the IS-LDPC codes exhibit excellent error-correcting performance and the proposed PAPR reduction scheme based on IS-LDPC codes significantly reduces the PAPR. Compared with the existing coding-based candidate generation schemes, the proposed scheme has a much lower searching complexity when the codeword is transmitted by multiple OFDM symbols. With all mentioned advantages, the proposed PAPR reduction scheme based on IS-LDPC codes could serve as an attractive PAPR reduction solution for future multicarrier communication systems.**

Index Terms—**Orthogonal frequency-division multiplexing (OFDM), peak-to-average power ratio (PAPR), low density parity-check codes (LDPC), progressive edge-growth (PEG).**

I. Introduction

Orthogonal frequency-division multiplexing (OFDM) has been widely adopted in various wireless communication standards, due to its capability to efficiently cope with frequency selective channels. However, one major drawback of OFDM systems is high peak-to-average power ratio (PAPR). High PAPR significantly complicates implementation of the radio frequency front-end, since power amplifiers with a wide linear range are required. Otherwise, the nonlinear characteristics of power amplifiers would distort the in-band signal and raise the out-of-band radiation. To reduce PAPR, many schemes have been proposed in the literature [1], [2], among which coding-based approaches have attracted considerable attentions due to their inherent error control capability and the simplicity of implementation. Particularly, coding-based approaches are classified into two categories in this paper: low PAPR coding and coding-based candidate generation schemes.

The low PAPR coding: it generates low PAPR codewords through coding. The low PAPR code was firstly proposed in [3]. In [4], the existence of asymptotically good codes with low PAPR was proven. In [5], efficient computation of the PAPR for any practical code was discussed. The Golay complementary sequences and Reed-Muller (RM) codes to achieve excellent PAPR performance were proposed in [6] and [7]. Later, a complement block-coding (CBC) scheme was proposed to reduce the PAPR in [8]. However, the error-correcting performance of these codes are quite far from the Shannon limit. In [9] and [10], time-frequency turbo block codes (TBC) were proposed to achieve good error-correcting performance as well as low PAPR, in which the frequency domain component code employs codes with low PAPR, like RM code or dual Bose-Ray-Chaudhuri code, and the time domain component code uses low density parity-check (LDPC) code. However, there are still apparent error-correcting performance gaps between the TBC codes and the capacity achieving codes.

The coding-based candidate generation schemes: it generates candidate codewords for any given codeword and a candidate with low PAPR is selected for transmission. In [17], candidates are generated by employing a scrambler before channel coding, therefore all candidates are also valid codewords. In [18], candidate codewords are generated with a number of interleavers before channel coding. Employment of random-like codes, such as turbo and LDPC code, were proposed in [19] and [20] to generate candidate codewords, which do not require an explicit scrambler/interleaver. Moreover, binary cyclic codes, Reed-Muller codes, Reed Solomon and simplex codes are considered in [21]–[23]. At first sight, the coding-based candidate generation schemes share the same principle of PAPR reduction with the selective mapping (SLM) [24] or partial transmit sequence (PTS) [25] schemes, which generate candidate signals and select a candidate of low PAPR for transmission. However, the major difference is that the candidates of the coding-based candidate generation schemes are valid codewords, while those of the SLM and PTS schemes are not necessarily valid codewords. Unlike the SLM and PTS schemes, the coding-based candidate generation schemes refrains from the use of explicit side information in the receiver, with the help of coding [17].

Compared with the low PAPR coding schemes, the coding-based candidate generation schemes do not suffer significant degradation of error-correcting performance, by employing error-correcting codes with proven performance [17]. Therefore, we focus on the coding-based candidate generation schemes in this paper. However, the existing coding-based candidate generation schemes do not support large number of candidates, due to the high complexity of searching the

Daiming Qu, Li Li and Tao Jiang (corresponding author) are with Department of Electronics and Information Engineering, Huazhong University of Science and Technology, Wuhan, 430074, China (e-mail: Tao.Jiang@ieee.org).

candidate with the lowest PAPR. Therefore, their PAPR reduction performance is limited, especially when one codeword is transmitted by multiple OFDM symbols, which will be further discussed in Section II.

In this paper, we first propose a code structure that enables each OFDM symbol to be independently treated for PAPR reduction, therefore the searching complexity is significantly reduced. Then, we propose a new family of LDPC codes, called as invertible subset LDPC (IS-LDPC) code, which complies with the proposed code structure. An IS-LDPC code has a number of disjoint invertible subsets, and each invertible subset can be independently inverted to generate candidates that are valid codewords of the LDPC code. To construct IS-LDPC codes with good error-correcting performance, we propose a modified progressive edge-growth construction algorithm, and verify its effectiveness by analyzing the girth and approximate cycle extrinsic message degree (ACE) [35] of the constructed Tanner graphs. Besides the excellent error-correcting performance and significant PAPR reduction, the proposed scheme supports multiple-OFDM-symbol frames very well, by dramatically reducing the searching complexity.

The remainder of this paper is organized as follows. In Section II, the proposed code structure for coding-based candidate generation schemes with low searching complexity is described. In Section III, we define the IS-LDPC codes and present several properties of the codes. The modified PEG construction algorithm are presented in Section IV. Then, we analyze the girth and ACE properties of the constructed IS-LDPC codes in Section V. PAPR reduction with the IS-LDPC codes is proposed in Section VI. Simulation results are presented in Section VII, followed by conclusions and future works in Section VIII.

Notations: Bold fonts are used to denote vectors; $[\cdot]^{\mathrm{T}}$ represents the transpose of a matrix; $\oplus$ denotes modulo 2 addition; $\overline{a}$ represents the negation of binary variable a, $\overline{\mathbf{A}}$ represents the negation of all bits of binary vector $\mathbf{A}$.

II. Proposed Code Structure with Low Searching Complexity

A. An example of coding-based candidate generation schemes

We briefly recall the PAPR reduction scheme proposed in [17] as a typical example of coding-based candidate generation schemes. At the transmitter of [17], U binary labels drive a scrambler to generate a scrambled output of the information bits, and the labels are inserted as a prefix. Then, the output is coded by an error control encoder and the coded bits are mapped onto OFDM subcarriers. The PAPR is reduced by choosing the proper labels. At the receiver, the labels can be easily recovered by decoding. One advantage of the coding-based candidate generation schemes is that they do not suffer significant degradation of error-correcting performance. Another advantage is that, the side information, which is called as label bits in [17], is embedded in codewords for transmission other than transmitted by an extra control channel. As a comparison, the side information of the SLM and PTS schemes is either transmitted by an extra control channel, or detected based on certain signal properties of the schemes [26]–[29], which incurs significant cost of overhead or computational complexity.

The major problem of the existing coding-based candidate generation schemes is the high complexity of searching the candidates with the lowest PAPR. For example, the scheme in [17] requires to search among 2^U different candidates to minimize the PAPR, which means a searching complexity of 2^U. This searching complexity is prohibitively high when U is large.

B. Multiple-OFDM-symbol frames

Most of the existing coding-based candidate generation schemes assume that a codeword is transmitted by a single OFDM symbol. However, a codeword is usually transmitted by multiple OFDM symbols in practical OFDM systems such as the well known IEEE 802.11a standard for Wireless Local Area Networks (WLAN) [34]. We call the multiple OFDM symbols, by which a single codeword is transmitted, as a multiple-OFDM-symbol frame in this paper.

Apparently, a coding-based candidate generation scheme should be able to effectively reduce the PAPRs of all OFDM symbols in a multiple-OFDM-symbol frame. Thus, U has to be much larger for a multiple-OFDM-symbol frame than that for a single OFDM symbol. Consequently, the searching complexity becomes a more severe issue when multiple-OFDM-symbol frame is considered.

C. Proposed code structure with low searching complexity

To lower the searching complexity for multiple-OFDM-symbol frames, we show in the followings how code structure affects the searching complexity, and propose a code structure with low searching complexity.

With coding-based candidate generation schemes, a new codeword is generated for a given codeword, when a label bit is flipped. The new codeword differs from the original one in a number of coded bits, which are marked with 'F' in Fig. 1. For the scheme in [17], the followings are observed: (1) the positions of the flipped coded bits depends on the information bits and other label bits; (2) the flipped coded bits are spread over multiple OFDM symbols, as shown in the upper part of Fig. 1. With this code structure, the PAPR of each OFDM symbol can not be independently treated, therefore searching among the entire set of candidate codewords is necessary, which means 2^U searching complexity.

To remedy the problem described above, we propose a code structure that enables low searching complexity for coding-based candidate generation schemes. The proposed code structure has the following properties: (1) for any given label bit, the positions of the flipped coded bits resulted from flipping the label bit are fixed, i.e., the positions do not depend on the information bits or other label bits; (2) there exists an assignment of coded bits to OFDM symbols, such that for each label bit, all flipped coded bits resulted from flipping the label bit are assigned to the same OFDM symbol, as illustrated in the lower part of Fig. 1. With the proposed code structure and proper bit assignment, the candidate codeword generated by flipping any given label bit differs from the original one

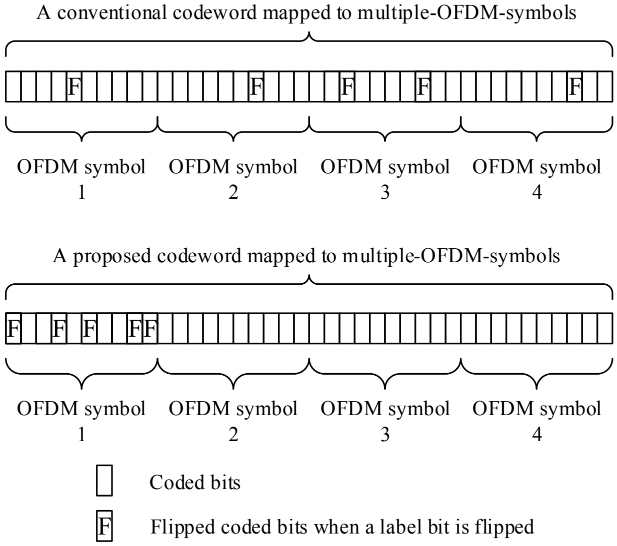

Fig. 1. The proposed code structure for coding-based candidate generation schemes with low searching complexity.

Original Codewords	Invert subset 1	Invert subset 2	Invert subset 1 & 2
000000	101010	010101	111111
000111	101101	010010	111000
001011	100001	011110	110100
001100	100110	011001	110011
010010	111000	000111	101101
010101	111111	000000	101010
011001	110011	001100	100110
011110	110100	001011	100001
100001	001011	110100	011110
100110	001100	110011	011001
101010	000000	111111	010101
101101	000111	111000	010010
110011	011001	100110	001100
110100	011110	100001	001011
111000	010010	101101	000111
111111	010101	101010	000000
$a_1a_2a_3a_4a_5a_6$	$a_1a_2a_3a_4a_5a_6$	$a_1a_2a_3a_4a_5a_6$	$a_1a_2a_3a_4a_5a_6$

Coded bits of invertible subset 1   Coded bits of invertible subset 2

Fig. 2. An example block code with two disjoint invertible subsets.

in only one OFDM symbol. In this case, the PAPR of each OFDM symbol can be independently treated by only varying its associated label bits. Therefore, instead of searching among the entire set of candidate codewords, only searching among a subset of candidate codewords is required, whose size is much smaller than 2^U. Specifically, consider the case that the frame consists of K OFDM symbols and each OFDM symbol is associated with U/K label bits, the searching complexity for each OFDM symbol is $2^{U/K}$ and total searching complexity for a codeword is reduced from 2^U to $K2^{U/K}$. The searching complexity reduction will be further discussed with examples in Section VI-C and VII-B. This complexity reduction is very huge when K is large, for multiple-OFDM-symbol frames.

To construct a code having good error-correcting performance and complying the proposed code structure, LDPC code is a good choice, due to the fact that LDPC code is among the best error-correcting codes known to date and rules of the proposed code structure could be applied in the constructions of LDPC codes. This idea leads to the proposed invertible subset LDPC code in the following section.

III. Proposed IS-LDPC Code

A. Definition of IS-LDPC code

Definition 1 (Invertible Subset): Let vector $\mathbf{A} = [a_1, a_2, \cdots, a_N]$ denote a codeword of binary linear block code $\mathcal{A}$, and subset $\mathcal{S} = \{i_1, i_2, \cdots, i_L\}$ denote a subset of indexes of the coded bits, i.e., $\{i_1, i_2, \cdots, i_L\} \subseteq \{1, 2, \cdots, N\}$. Subset $\mathcal{S}$ is an invertible subset if, for any valid codeword $\mathbf{A}$ of $\mathcal{A}$, codeword $\widetilde{\mathbf{A}} = [\widetilde{a}_1, \widetilde{a}_2, \cdots, \widetilde{a}_N]$ is a valid codeword of $\mathcal{A}$, where

$$\widetilde{a}_i = \begin{cases} \overline{a}_i, & i \in \mathcal{S} \\ a_i, & \text{otherwise} \end{cases}. \tag{1}$$

An example block code of two disjoint invertible subsets is shown in Fig. 2, which has six coded bits and 16 valid codewords. All valid codewords of the block code are presented in the leftmost block. It is observed that, for any given codeword, the codewords generated by only inverting subset 1, only inverting subset 2, and inverting both subsets, are valid codewords of the block code.

A binary LDPC code is defined by a sparse parity-check matrix $\mathbf{H}$ having dimension $M \times N$ or its equivalent Tanner graph [11]–[16]. Let $(\mathcal{V}, \mathcal{C}, \mathcal{E})$ denote the Tanner graph of the LDPC code, where $\mathcal{V} = \{v_1, v_2, \cdots, v_N\}$ is the variable-node set, $\mathcal{C} = \{c_1, c_2, \cdots, c_M\}$ is the check-node set, and $\mathcal{E}$ is the set of edges ($\mathcal{E} \subseteq \mathcal{V} \times \mathcal{C}$), with edge $(v_j, c_i) \in \mathcal{E}$ if and only if $h_{i,j} \neq 0$, where $h_{i,j}$ denotes the entry of $\mathbf{H}$ at the ith row ($1 \leq i \leq M$) and the jth column ($1 \leq j \leq N$). In this paper, we consider irregular LDPC codes with variable node and check node degree distributions defined by the polynomials as follows,

$$\lambda(x) = \sum_{i=2}^{d_{v_{max}}} \lambda_i x^{i-1}, \quad \text{and} \quad \rho(x) = \sum_{i=2}^{d_{c_{max}}} \rho_i x^{i-1}, \tag{2}$$

where $d_{v_{max}}$ and $d_{c_{max}}$ are the maximum variable and check node degree of the code, respectively. λ_i and ρ_i represent the fraction of edges emanating from degree i variable and check nodes, respectively.

Definition 2 (IS-LDPC codes of inversion freedom U): An invertible subset LDPC (IS-LDPC) code of inversion freedom U is an LDPC code with U invertible subset, and there is no intersection among different invertible subsets.

According to the above definitions, if an IS-LDPC code has multiple disjoint invertible subsets, these subsets can be inverted independently, and all generated codewords are valid codewords.

Actually, all LDPC codes have inversion freedoms no less than one, since it is easy to find at least one invertible subset for any LDPC codes by the following way: given any non-zero LDPC codeword, the set of the indexes of the non-zero coded bits forms an invertible subset of the LDPC code. However, the challenge is that, for practical use of IS-LDPC codes in communication systems, the following requirements have to be satisfied: (1) the inversion freedom is greater than the number of OFDM symbols in a frame, and greater inversion freedom is required for lower PAPR; (2) the number of coded bits for each invertible subset can be specified by the systems; (3) the indexes of coded bits for each invertible subsets can be specified by the systems, i.e., $\{i_1, i_2, \cdots, i_L\}$ can be specified for invertible subset $\mathcal{S}$.

It will be shown in Section VI-C that, IS-LDPC codes satisfying the above requirements could comply with the code structure proposed in Section II-C.

B. Properties of IS-LDPC parity-check matrices and Tanner graphs

Let $\mathcal{S}_{\text{IS}}$ denote an invertible subset, and vector $\mathbf{A}_{\text{IS}}$ denote the corresponding coded bits. Let $\mathcal{S}_{\text{OT}}$ denote the subset of the coded bits that do not belong to $\mathcal{S}_{\text{IS}}$, and vector $\mathbf{A}_{\text{OT}}$ denote the corresponding coded bits. Note that, other invertible subsets could be included in $\mathcal{S}_{\text{OT}}$. The coded bits are reordered such that the codeword $\mathbf{A} = [\mathbf{A}_{\text{IS}}, \mathbf{A}_{\text{OT}}]$. Similarly, the variable-node set $\mathcal{V}$ is partitioned into two subsets $\mathcal{V}_{\text{IS}}$ and $\mathcal{V}_{\text{OT}}$, where $\mathcal{V}_{\text{IS}}$ and $\mathcal{V}_{\text{OT}}$ corresponds to $\mathcal{S}_{\text{IS}}$ and $\mathcal{S}_{\text{OT}}$, respectively. As a Tanner graph defines a parity-check matrix, the parity-check matrix $\mathbf{H}$ also consists of two submatrices, i.e., $\mathbf{H} = [\mathbf{H}_{\text{IS}}, \mathbf{H}_{\text{OT}}]$, where $\mathbf{H}_{\text{IS}}$ and $\mathbf{H}_{\text{OT}}$ are submatrices of $\mathbf{H}$, and the columns of $\mathbf{H}_{\text{IS}}$ and $\mathbf{H}_{\text{OT}}$ correspond to the variable nodes in subset $\mathcal{V}_{\text{IS}}$ and $\mathcal{V}_{\text{OT}}$, respectively.

Theorem 1: A necessary and sufficient condition for $\mathcal{S}_{\text{IS}}$ to be an invertible subset of the LDPC code is that, each row of $\mathbf{H}_{\text{IS}}$ has even Hamming weight, i.e., $\mathbf{H}_{\text{IS}}[1, 1, \cdots, 1]^T = \mathbf{0}$ over GF(2).

Proof: Let $\mathcal{S}_{\text{S}}$ denote a subset and $\mathcal{S}_{\text{S}} \subseteq \{1, 2, \cdots, N\}$, vector $\mathbf{A}_{\text{S}}$ denote its corresponding coded bits and matrix $\mathbf{H}_{\text{S}}$ denotes its corresponding submatrix of $\mathbf{H}$. We can write over GF(2), for any $\mathcal{S}_{\text{S}}$,

$$\begin{aligned} &\mathbf{H}_{\text{S}}[\mathbf{A}_{\text{S}}]^{\text{T}} + \mathbf{H}_{\text{S}}[\overline{\mathbf{A}_{\text{S}}}]^{\text{T}} \\ &= \mathbf{H}_{\text{S}}[\mathbf{A}_{\text{S}} + \overline{\mathbf{A}_{\text{S}}}]^{\text{T}} \\ &= \mathbf{H}_{\text{S}}[1, 1, \ldots, 1]^{\text{T}}. \end{aligned} \tag{3}$$

(1) Proof of the necessary condition.

Let $\widetilde{\mathbf{A}} = [\overline{\mathbf{A}_{\text{IS}}}, \mathbf{A}_{\text{OT}}]$, then we have

$$\begin{aligned} &\mathbf{H}[\widetilde{\mathbf{A}}]^{\text{T}} + \mathbf{H}[\mathbf{A}]^T \\ &= \mathbf{H}_{\text{IS}}[\overline{\mathbf{A}_{\text{IS}}}]^{\text{T}} + \mathbf{H}_{\text{OT}}[\mathbf{A}_{\text{OT}}]^{\text{T}} + \mathbf{H}_{\text{IS}}[\mathbf{A}_{\text{IS}}]^{\text{T}} + \mathbf{H}_{\text{OT}}[\mathbf{A}_{\text{OT}}]^{\text{T}} \\ &= \mathbf{H}_{\text{IS}}[\overline{\mathbf{A}_{\text{IS}}}]^{\text{T}} + \mathbf{H}_{\text{IS}}[\mathbf{A}_{\text{IS}}]^{\text{T}} \\ &= \mathbf{H}_{\text{IS}}[1, 1, \ldots, 1]^{\text{T}}. \end{aligned} \tag{4}$$

Note that, if $\mathcal{S}_{\text{IS}}$ is an invertible subset, and $\widetilde{\mathbf{A}}$ is generated from $\mathbf{A}$ by inverting $\mathbf{A}_{\text{IS}}$, $\widetilde{\mathbf{A}}$ is a valid codeword of the LDPC code. Then, $\mathbf{H}[\widetilde{\mathbf{A}}]^{\text{T}} = \mathbf{H}[\mathbf{A}]^T = \mathbf{0}$, and

$$\mathbf{H}[\widetilde{\mathbf{A}}]^{\text{T}} + \mathbf{H}[\mathbf{A}]^T = \mathbf{0}. \tag{5}$$

Therefore,

$$\mathbf{H}_{\text{IS}}[1, 1, \ldots, 1]^{\text{T}} = \mathbf{0}. \tag{6}$$

In another words, $\mathbf{H}_{\text{IS}}$ is a matrix of even Hamming weight per row.

(2) Proof of the sufficient condition.

Since each row of $\mathbf{H}_{\text{IS}}$ has even Hamming weight,

$$\mathbf{H}_{\text{IS}}[1, 1, \cdots, 1]^T = \mathbf{0}. \tag{7}$$

According to (3), we have $\mathbf{H}_{\text{IS}}[\mathbf{A}_{\text{IS}}]^{\text{T}} + \mathbf{H}_{\text{IS}}[\overline{\mathbf{A}_{\text{IS}}}]^{\text{T}} = \mathbf{H}_{\text{IS}}[1, 1, \cdots, 1]^T = \mathbf{0}$, i.e.,

$$\mathbf{H}_{\text{IS}}[\mathbf{A}_{\text{IS}}]^{\text{T}} = \mathbf{H}_{\text{IS}}[\overline{\mathbf{A}_{\text{IS}}}]^{\text{T}}. \tag{8}$$

Then, we have

$$\begin{aligned} \mathbf{H}[\widetilde{\mathbf{A}}]^{\text{T}} &= \mathbf{H}_{\text{IS}}[\overline{\mathbf{A}_{\text{IS}}}]^{\text{T}} + \mathbf{H}_{\text{OT}}[\mathbf{A}_{\text{OT}}]^{\text{T}} \\ &= \mathbf{H}_{\text{IS}}[\mathbf{A}_{\text{IS}}]^{\text{T}} + \mathbf{H}_{\text{OT}}[\mathbf{A}_{\text{OT}}]^{\text{T}} \\ &= \mathbf{H}[\mathbf{A}]^T \\ &= \mathbf{0}. \end{aligned} \tag{9}$$

The above equality means that $\widetilde{\mathbf{A}}$ is a valid codeword under the parity-check matrix $\mathbf{H}$. Therefore, $\mathcal{S}_{\text{IS}}$ is an invertible subset. ■

Examining the theorem in terms of Tanner graph, the following remarks is reached.

Remark 1: A necessary and sufficient condition for $\mathcal{S}_{\text{IS}}$ to be an invertible subset of the LDPC code is that, for any check node, the total number of edges connecting the check node to all variable nodes in $\mathcal{V}_{\text{IS}}$ is even.

Remark 2: It is inferred from Remark 1 that if $\mathcal{S}_{\text{IS}}$ is an invertible subset, the total number of edges emanating from $\mathcal{V}_{\text{IS}}$ is even.

Since disjoint invertible subsets of an IS-LDPC code can be inverted independently, Theorem 1 can be straightforwardly generalized to multiple invertible subsets:

Remark 3: A necessary and sufficient condition for U disjoint subsets of coded bits to be invertible subsets of the LDPC code is that, for any pair of the check node and subset, the total number of edges connecting the check node and all variable nodes of the subset is even.

IV. CONSTRUCTION OF IS-LDPC CODES

This section discusses the construction of IS-LDPC codes with disjoint invertible subsets that are specified in advance.

It has been proven that the PEG algorithm [13] is a powerful algorithm to construct LDPC codes. The PEG algorithm builds up a Tanner graph in an edge-by-edge manner, in which the local girth of a variable node is maximized whenever a new edge is grown for it. Particularly, when growing a new edge for variable node v_j, the PEG algorithm expands a tree subgraph from v_j up to depth l so that the cardinality of $\mathcal{N}_{v_j}^l$ stops increasing but is less than M, or $\overline{\mathcal{N}}_{v_j}^l \neq \emptyset$ but $\overline{\mathcal{N}}_{v_j}^{l+1} = \emptyset$ ($\mathcal{N}_{v_j}^l$ and $\overline{\mathcal{N}}_{v_j}^l$ denote the set of check nodes reached by the expansion from variable node v_j up to depth l, and its complement, respectively), then a check node in the set $\overline{\mathcal{N}}_{v_j}^l$ with the minimum current check-node degree is chosen to be connected to v_j. For details of the PEG algorithm, please refer to [13].

Algorithm 1 IS-PEG algorithm

for $j = 1$ to N **do**
  for $k = 1$ to d_{v_j}, where d_{v_j} represents the degree of variable node v_j, **do**
    if $k = 1$ **then**
      Update $\mathcal{O}$, P and Q.
      if $v_j \in \mathcal{V}_{\text{IS}}$ and $P < Q$ **then**
        $\mathcal{E}_{v_j}^1 \leftarrow$ edge (v_j, c), where c is a check node such that it has the lowest check-node degree under the current graph setting $\mathcal{E} = \mathcal{E}_{v_1} \cup \cdots \cup \mathcal{E}_{v_{j-1}}$,
      else
        $\mathcal{E}_{v_j}^1 \leftarrow$ edge (v_j, c), where c is a check node from $\mathcal{O}$ such that it has the lowest check-node degree under the current graph setting $\mathcal{E} = \mathcal{E}_{v_1} \cup \cdots \cup \mathcal{E}_{v_{j-1}}$,
      end if, where $\mathcal{E}_{v_i}$ contains all edges grown for v_i, i.e., $\mathcal{E}_{v_i} = \mathcal{E}_{v_i}^1 \cup \mathcal{E}_{v_i}^2 \cup \cdots$, and $\mathcal{E}_{v_i}^m$ is the mth edge grown for v_i.
    else
      Update $\mathcal{O}$, P and Q.
      Expand a tree subgraph from variable node v_j up to depth l under the current graph setting $\mathcal{E} = \mathcal{E}_{v_1} \cup \cdots \cup \mathcal{E}_{v_j}$, such that the cardinality of $\mathcal{N}_{v_j}^l$ stops increasing but is less than M, or $\overline{\mathcal{N}}_{v_j}^l \neq \emptyset$ but $\overline{\mathcal{N}}_{v_j}^{l+1} = \emptyset$. Then, the set of check-node candidates $\mathcal{N}$ is
      if $v_j \in \mathcal{V}_{\text{IS}}$ and $P < Q$ **then**
        $\mathcal{N} = \overline{\mathcal{N}}_{v_j}^l$,
      else
        $\mathcal{N} = \overline{\mathcal{N}}_{v_j}^l \cap \mathcal{O}$.
      end if
      $\mathcal{E}_{v_j}^k \leftarrow$ edge (v_j, c), where c is a check node in $\mathcal{N}$, which has the lowest check-node degree.
    end if
  end for
end for

In this subsection, we propose a modified PEG algorithm, which is called as IS-PEG algorithm, to construct IS-LDPC codes. The IS-PEG algorithm is based on Theorem 1 and the Remarks in Section III, i.e., it ensures that, for any pair of check node and invertible subset, the total number of edges connecting the check node to all variable nodes of the invertible subset is even. For simplicity of presentation, we consider in the followings the construction of an IS-LDPC code with $U = 1$, i.e., only one invertible subset is specified for the code. The extension to multiple invertible subsets is straightforward: as indicated by Remark 3, the invertible subsets independently satisfy Theorem 1, therefore the proposed algorithm could be performed alternately and independently on these subsets.

The key idea of the IS-PEG algorithm is that: (1) the earlier edges grown for $\mathcal{V}_{\text{IS}}$ (the variable node set of the invertible subset) are grown following the same rule as that of the PEG algorithm; (2) the later edges grown for $\mathcal{V}_{\text{IS}}$ are forced to connect to the check nodes that are connected to $\mathcal{V}_{\text{IS}}$ odd times.

The IS-PEG algorithm presented in Algorithm 1 is explained briefly as follows. When a new edge is to be grown for the variable node $v_j \in \mathcal{V}_{\text{IS}}$, let $\mathcal{O}$ denote the current set of check nodes that are connected to $\mathcal{V}_{\text{IS}}$ odd times, P denote the number of check nodes in $\mathcal{O}$, Q denote the total number of edges remained to be grown for all variable nodes in $\mathcal{V}_{\text{IS}}$, and $\mathcal{N}$ denote the set of check-node candidates for this edge. If $P < Q$, let $\mathcal{N} = \overline{\mathcal{N}}_{v_j}^l$, otherwise, let $\mathcal{N}$ be the intersection of $\mathcal{O}$ and $\overline{\mathcal{N}}_{v_j}^l$, i.e.,

$$\mathcal{N} = \begin{cases} \overline{\mathcal{N}}_{v_j}^l, & P < Q \\ \overline{\mathcal{N}}_{v_j}^l \cap \mathcal{O}, & \text{otherwise} \end{cases}, \tag{10}$$

where $\overline{\mathcal{N}}_{v_j}^l$ is the complement of the set of check nodes reached by the tree expansion from variable node v_j up to depth l. Eq. (10) means that the edge is grown exactly the same way as it is in the original PEG algorithm when $P < Q$; otherwise, the edge is forced to connect to the check nodes that are connected to $\mathcal{V}_{\text{IS}}$ odd times, which decreases P by one. Iteratively performing the forced connecting eventually leads to $P = Q = 0$, which means that every check node is connected to $\mathcal{V}_{\text{IS}}$ even times.

Before running the IS-PEG algorithm, we should make sure that the total number of edges to be grown for $\mathcal{V}_{\text{IS}}$ is even, due to Remark 2. If this is not satisfied, we could simply decrease by one the degree of one variable node with the highest degree in $\mathcal{V}_{\text{IS}}$, which would only lead to a slightly different variable-node degree distribution compared with the original one. When running the IS-PEG algorithm, one situation may happen: there is no check node in the intersection of the two sets, i.e., $\overline{\mathcal{N}}_{v_j}^l \cap \mathcal{O} = \emptyset$. In this case, check nodes are selected in $\overline{\mathcal{N}}_{v_j}^{l-1} \cap \mathcal{O}$ instead.

Similar to the PEG algorithm for systematic LDPC codes, all variable nodes are sorted in nondecreasing order with respect to their degrees, i.e, $d_{v_1} \leq d_{v_2} \leq \cdots \leq d_{v_N}$, and v_{N-M+1} to v_N correspond to the information bits, where d_{v_j} represents the degree of variable node v_j.

V. Girth and ACE Analysis of the Constructed IS-LDPC Tanner Graph

With the forced connecting described in Algorithm 1, it is clear that short cycles of length four can not be avoided in the Tanner graph. In this section, we consider the effects of these four-cycles by analyzing the girth [13] and approximate cycle extrinsic message degree (ACE) [35], [38] of the Tanner graphs.

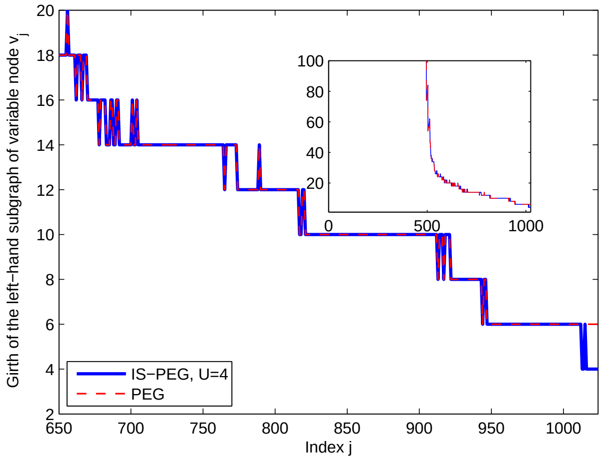

Fig. 3. Girth of the left-hand subgraphs of variable node v_j for the PEG and IS-PEG Tanner graph, with $N = 1024, R = 1/2, d_{v_{max}} = 15, U = 4$.

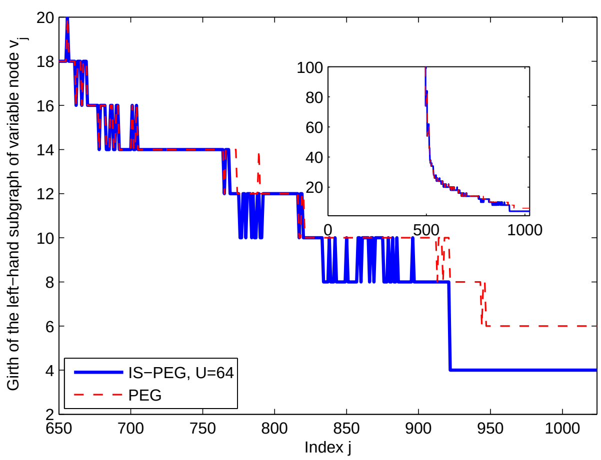

Fig. 4. Girth of the left-hand subgraphs of variable node v_j for the PEG and IS-PEG Tanner graph, with $N = 1024, R = 1/2, d_{v_{max}} = 15, U = 64$.

In the following examples, IS-LDPC codes of length $N = 1024$ and rate $R = 1/2$ are constructed. The IS-LDPC codes and the LDPC code constructed by the PEG algorithm employ the same degree distribution pair, which is optimized by the density evolution technique [12], with maximum variable node degree $d_{v_{max}} = 15$. The variable-node set $\mathcal{V}$ is partitioned into U disjoint variable-node subsets, denoted as $\mathcal{V}_1, \mathcal{V}_2, \cdots, \mathcal{V}_U$, where $\mathcal{V}_u$ corresponds to the invertible subset $\mathcal{S}_u$. Uniformly interleaved partition is adopted for the subsets, i.e., $\mathcal{S}_u = \{u, u+U, \cdots, N-U+u\}$, for $u = 1, 2, \cdots, U$.

A. Girth of the left-hand subgraph

Girth of the left-hand subgraph is a powerful tool to investigate the properties of cycles, and it gives an insight on the error performance of a constructed LDPC code [13]. The left-hand subgraph of variable node v_j consists of the variable nodes $v_1, v_2, ..., v_j$, $1 \leq j \leq N$, the edges that emanate from them, and the check nodes they are connected to. It is desirable, in particular for irregular LDPC codes, that the girth of the left-hand subgraph of v_j decreases slowly as a function of j, so that the possibility that lower degree nodes together form a small cycle decreases [13]. The PEG algorithm is actually an algorithm that tries to maximize the girth of the left-hand subgraph. Fig. 3 depicts the girth of the left-hand subgraph of variable node v_j as a function of j for Tanner graphs constructed by the PEG and IS-PEG algorithm ($U = 4$ for IS-PEG). To show details of the variation, we present the result for $650 \leq j \leq 1024$ in Fig. 3. The girth of the left-hand subgraph for all variable nodes is embedded in the figure. Similarly, the result for $U = 64$ are presented in Fig. 4. From these figures, the followings are observed.

- The curves of IS-PEG algorithm and those of PEG algorithm decrease slowly as a function of j. Thus, the IS-PEG construction also possesses the desired property that, the possibility that lower degree variable nodes together form a short cycle decreases.
- Although four-cycles are formed in the IS-PEG Tanner graph, all these short cycles include high-degree variable nodes. The reason is that the forced connecting in the IS-PEG algorithm only happens for high-degree variable nodes.
- The curve of the IS-PEG algorithm decreases more quickly for larger U.

B. ACE Metric

It is well known that not all short cycles are equally harmful, and the connectivity of a short cycle with the rest of the graph should also be taken into account. Tian *et al.* [35] proposed the ACE metric to measure the level of connectivity of a cycle with the rest of the graph. Then, the ACE metric is widely adopted in LDPC code construction [35]–[38]. In addition, the ACE metric is also used as an efficient tool to evaluate the performance of finite-length LDPC codes [38]. The ACE of a cycle is defined as the following [35].

Definition 3 (ACE): The ACE of a length $2l$ cycle is $\sum_k (d_{v(k)} - 2)$, where $v(k)$ represents the kth variable node in this cycle and $d_{v(k)}$ denotes its degree.

The ACE metric of variable node v, is defined as the minimum ACE of all cycles that involve v and are shorter than a given length [35]. In this paper, we use the ACE metric of cycles shorter than eight to evaluate the IS-PEG algorithm.

In the simulation of Fig. 5, we calculate the ACE metric for all variable nodes and present the distribution of ACE metric by a histogram, for the codes constructed by the PEG and IS-PEG algorithms. The followings are observed from the figure.

- The minimum ACE metric is 13 for the PEG algorithm, and it decreases to 12 for the IS-PEG algorithm, which is a slight degradation.
- The number of variable nodes having ACE metric of 12 increases with U.
- The ACE metrics of the IS-PEG algorithm are mainly distributed between 13 and 17 as those of the PEG

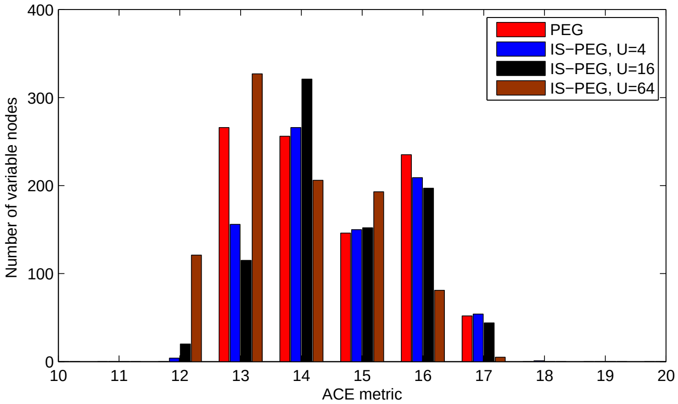

Fig. 5. Distribution of ACE metric of the PEG and IS-PEG constructed codes, for cycles shorter than eight, with $N = 1024$, $R = 1/2$, $d_{v_{max}} = 15$.

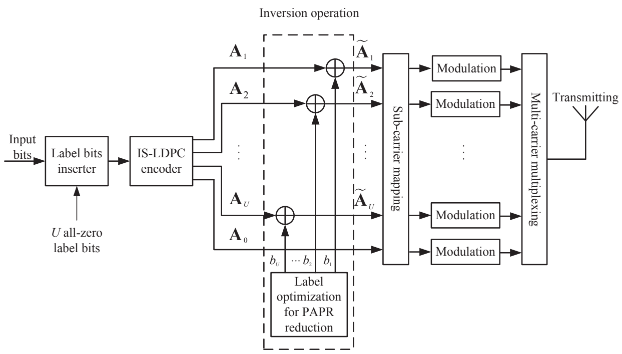

Fig. 6. Transmitter of the OFDM system with IS-LDPC codes for PAPR reduction.

algorithm, even for $U = 64$.

Based on the above analysis, we anticipate that the error-correcting performance of the example IS-LDPC codes ($N = 1024$, $R = 1/2$) would be close to that of the corresponding LDPC codes constructed by the original PEG algorithm, for $U = 4$ and 16. As for $U = 64$, since there are too many short cycles and variable nodes of ACE metric 12, the error-correcting performance of the example IS-LDPC code would suffer a clear degradation.

VI. PAPR Reduction with Low Complexity

A. PAPR reduction Based on IS-LDPC codes

The transmitter of the OFDM system with an IS-LDPC code for PAPR reduction is illustrated in Fig. 6. After the IS-LDPC encoding, the coded bits are reordered and grouped based on the U invertible subsets, such that $\mathbf{A} = [\mathbf{A}_0, \mathbf{A}_1, \cdots, \mathbf{A}_U]$, where sub-vector $\mathbf{A}_u$ $(1 \leq u \leq U)$ represents the coded bits of the uth invertible subset $\mathcal{S}_u$, and sub-vector $\mathbf{A}_0$ represents the other coded bits. Sub-vector $\mathbf{A}_0$ exists if there are some coded bits that do not belong to any of the invertible subsets.

Let $\widetilde{\mathbf{A}}_u$ denote the sub-vector after the inversion operation, for $u = 1, 2, \cdots, U$, and the codeword after the inversion operation is denoted as $\widetilde{\mathbf{A}} = [\mathbf{A}_0, \widetilde{\mathbf{A}}_1, \cdots, \widetilde{\mathbf{A}}_U]$. For the binary IS-LDPC code, the inversion operation could be realized by XOR operation as

$$\widetilde{\mathbf{A}}_u = \mathbf{A}_u \oplus [\underbrace{b_u, \ldots, b_u}_{L_u}], \text{ for } u = 1, 2, \cdots, U, \tag{11}$$

where L_u is the length of the uth invertible subset, and label $b_u \in \{0, 1\}$ determines whether subset u is inverted ($u = 1, 2, \cdots, U$), i.e., $\mathbf{A}_u$ is inverted when $b_u = 1$, otherwise, $\mathbf{A}_u$ is not inverted. Since each invertible subset can be inverted independently, $\widetilde{\mathbf{A}}$ is a valid codeword no matter what vector $[b_1, \cdots, b_U]$ is employed at the transmitter. Then, the coded bits of $\widetilde{\mathbf{A}}$ are mapped onto a number of subcarriers, modulated into phase-shift keying (PSK) or quadrature-amplitude modulation (QAM) symbols. Finally, the transmitted signal is formed by multicarrier multiplexing.

The label optimization module shown in Fig. 6 generates a proper vector $[b_1, \cdots, b_U]$, so that PAPR of the transmitted signal is lowered. Since each invertible subset can be independently inverted, the original codeword $\mathbf{A}$ can be transformed into 2^U different candidates (including $\mathbf{A}$ itself). For the ideal case, the candidate codeword corresponding to the time signal with the minimum PAPR is selected for transmission. In this way, the PAPR is significantly reduced, especially when the inversion freedom U is high. It is worth mentioning that the inversion operation is very similar to the phase rotation in the PTS scheme [25], if the invertible subsets are mapped onto the sign bits of subcarriers. If this is the case, the methods for phase optimization in the PTS scheme [30]–[33] could be directly employed for label optimization in the proposed scheme.

To tell whether the subsets are inverted, the labels $[b_1, \cdots, b_U]$ have to be transmitted along with the codeword. Fig. 6 depicts a method to encode and transmit the labels, in which U zero label bits are appended to the information bits before encoding. In addition, the IS-LDPC encoder employs systematic encoding, and the IS-LDPC code is constructed such that each invertible subset has exactly one label bit. In this way, each invertible subset consists of one label bit, a number of information bits and parity bits. If a subset is inverted, its label bit is flipped, and so are its information bits. Obviously, the label bit of subset u equals to b_u after inversion operation at the transmitter, and it serves as an indication of whether the corresponding information bits are inverted. Therefore, the receiver could use the decoded label bit to recover its associated information bits.

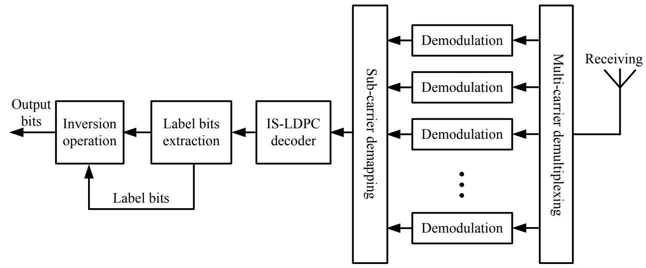

Fig. 7. Receiver of the OFDM system with IS-LDPC codes.

Fig. 7 presents the receiver diagram of the OFDM system.

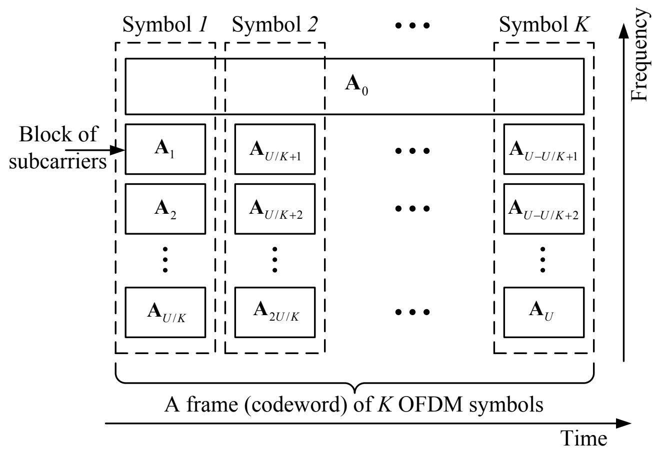

Fig. 8. An example of an IS-LDPC codeword transmitted by K OFDM symbols.

After multicarrier demultiplexing, demodulation and subcarrier demapping, the transmitted codeword $\widetilde{\mathbf{A}}$ is recovered by the IS-LDPC decoder, which is a standard LDPC decoder. Then, the label bits are extracted from $\widetilde{\mathbf{A}}$, and the original codeword $\mathbf{A}$ is recovered as

$$a_i = \begin{cases} \widetilde{a}_i \oplus b_u, & \text{if } i \in \mathcal{S}_u \text{ and } u = 1, 2, \cdots, U \\ \widetilde{a}_i, & \text{otherwise} \end{cases}, \tag{12}$$

where $\widetilde{a}_i$ is the ith bit of $\widetilde{\mathbf{A}}$.

B. Code rate

Due to the transmission of label bits, the effective code rate R_{E} (number of information bits over length of codeword) for the IS-LDPC code is $(RN - U)/N$, where R is the nominal code rate of the IS-LDPC code. If this rate loss is not to be accepted, we recommend the following modification to the transmitter described above: (1) let the number of the information bits and label bits be RN and U, respectively; (2) construct an IS-LDPC code of inversion freedom U, with code length $N+U$ and nominal code rate $(RN+U)/(N+U)$; (3) encode the information bits and all-zero label bits as Fig. 6; (4) puncture U bits in the codeword. The receiver should be modified accordingly. With these modifications, the effective code rate is still R, and the transmitted codeword length is still N. The bit-positions for the punctured bits could be randomly selected by the system in advance. We will compare the proposed system with the conventional LDPC-coded OFDM system in terms of error performance, under the same effective code rate, in Section VII.

C. Low searching complexity

As discussed in Section II-C, assignment of coded bits to OFDM symbols should ensure that, for each invertible subset, its coded bits are assigned to the same OFDM symbol. Fig. 8 shows an example frame structure that satisfies this requirement, in which a codeword is transmitted by K OFDM symbols. The IS-LDPC code in the example has U disjoint invertible subsets, and $\mathbf{A}_1, \mathbf{A}_2, \cdots, \mathbf{A}_U$ represent the coded bits that belong to the invertible subset $1, 2, \cdots, U$, respectively, and $\mathbf{A}_0$ represents the other coded bits. As shown in Fig. 8, each OFDM symbol is assigned with U/K complete invertible subsets and part of $\mathbf{A}_0$, where U/K is assumed to be an integer. With this assignment, the proposed scheme complies with the code structure proposed in Section II. In this way, the PAPR of each OFDM symbol can be independently reduced by the inversion operation on its U/K invertible subsets. Obviously, searching among $2^{U/K}$ different candidates is required to minimize the PAPR of each OFDM symbol. Thus, the total number of searching is $K2^{U/K}$ to minimize the PAPR of all symbols in the frame, which is dramatically lower than 2^U when K is large.

VII. Simulation Results

A. Error-correcting performance

In this subsection, we demonstrate the error-correcting performance of the IS-LDPC codes by computer simulation. The code rate is set to $1/2$ or $3/4$. The degree distribution pairs for the IS-LDPC and LDPC codes are identical, which are optimized by the density evolution technique [12], [39], with the maximum variable node degree $d_{v_{max}} = 15$. The highest degree node of each invertible subset is selected to be the label bit node in the code construction, which ensures quick and reliable recovery of the label bits in decoding [40]. QPSK modulation is employed at the transmitter. Note that, since the proposed IS-LDPC code is binary, there is no limitation on the modulation type, with which it works. The receiver employs a standard log-likelihood ratio belief propagation (LLR-BP) decoder with a maximum of 80 decoding iterations.

The aim of Fig. 9 is to demonstrate the error-correcting capability of IS-LDPC code itself. Therefore, no subset inversion is applied and all label bits are employed to convey information bits. Fig. 9 presents bit error rate (BER) performance of the IS-LDPC codes constructed by the IS-PEG algorithm, with different N, R and U, over AWGN channel. It is well known that PEG constructed LDPC codes have excellent error-correcting performance, especially for short-block-length LDPC codes, therefore its BER performance is also presented for comparison. It is observed that the error-correcting performance of the IS-LDPC codes is very close to that of the corresponding LDPC codes constructed by PEG, when $U <= 32$ for $R = 1/2$ and $N = 1024$, which is in accordance with the analysis and prediction in Section IV. A clear error-correcting performance degradation is observed when $U = 64$ for $R = 1/2$ and $N = 1024$. Nevertheless, IS-LDPC codes with longer codeword length can sustain higher inversion freedom without significant performance degradation. This is also verified in Fig. 9, where the performance degradation is negligible when $U = 64$ for $R = 1/2$ and $N = 2048$. In the case of $R = 3/4$, there is no significant degradation even when $U = 64$ for $N = 1024$, and when $U = 128$ for $N = 2048$.

The simulations of Fig. 10 and Fig. 11 are to demonstrate the error-correcting capability of the IS-LDPC code in an

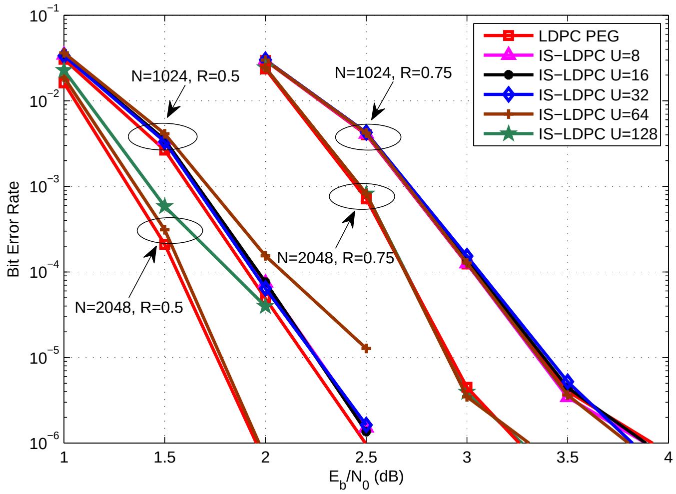

Fig. 9. BER performance of the IS-LDPC codes over AWGN channel, with $U = 8, 16, 32, 64$ for $N = 1024$ and $U = 64, 128$ for $N = 2048$. The aim of the simulation is to demonstrate the error-correcting capability of IS-LDPC code itself. Therefore, no subset inversion is applied and all label bits are employed to convey information bits.

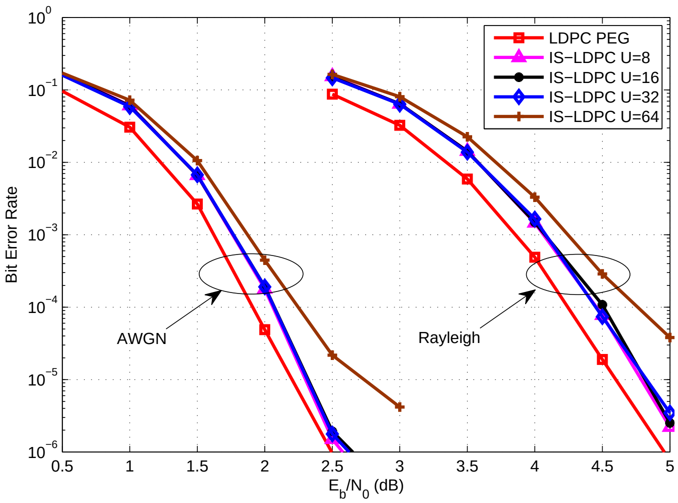

Fig. 10. BER performance of the punctured IS-LDPC codes, with effective code rate $R_{\mathrm{E}} = 1/2$ and $N = 1024$, over AWGN and uncorrelated Rayleigh channel. The subset inversion is applied.

OFDM system with subset inversion. To compare the IS-LDPC and LDPC codes with the same effective code rates, the punctured IS-LDPC codes described in Section VI-B is employed in the simulation. Fig. 10 presents the BER performance of the IS-LDPC codes with $N = 1024$, effective code rate $R_{\mathrm{E}} = 1/2$, and different U, over AWGN and uncorrelated Rayleigh fading channel. It is observed that there is a clear gap between the BER performance of IS-LDPC codes and the corresponding PEG constructed LDPC code. This gap is caused by the error propagation that occurs with fail-decoded label bits and wrong inversion of their information bits at the receiver. Nevertheless, the BER performance loss between the IS-LDPC code and corresponding LDPC code is less than 0.2 dB at BER of 10^{-5}, when $U \leq 32$. Since frame error rate (FER) performance is more important than BER performance for wireless communications under fading channels, Fig. 11 presents FER

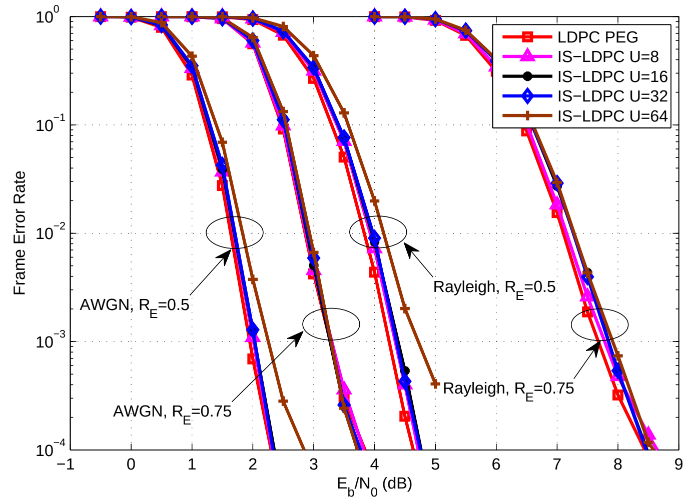

Fig. 11. FER performance of the punctured IS-LDPC codes, with $N = 1024$, over AWGN and uncorrelated Rayleigh channel. The subset inversion is applied.

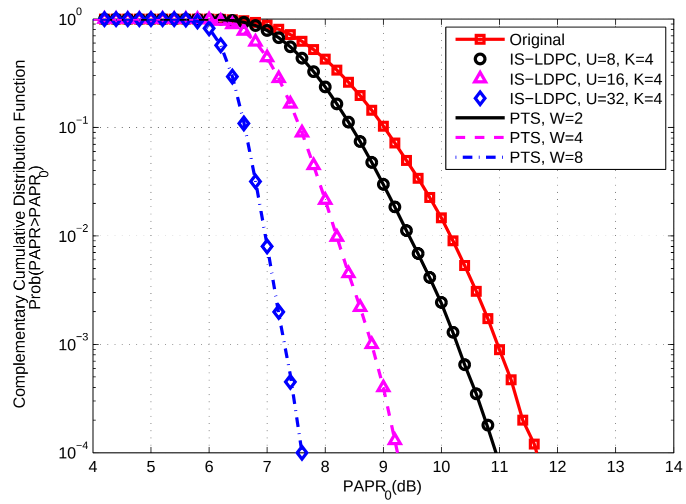

Fig. 12. PAPR performance of the OFDM system with the proposed PAPR reduction scheme based on IS-LDPC codes.

performance of the IS-LDPC codes with $N = 1024$, different R_{E} and U, over AWGN channel and uncorrelated Rayleigh fading channel. It is observed that there is no significant FER performance loss for IS-LDPC codes when $U \leq 32$, over AWGN channel. The FER performance loss is slightly increased when the uncorrelated Rayleigh fading channel is applied, which is about 0.2 dB at FER of 10^{-2} when $U = 32$.

Based on the above simulation results, we conclude that the proposed scheme exhibits excellent error performance, which is very close to that of LDPC codes constructed by the PEG algorithm, for a wide range of U.

B. Searching complexity and PAPR performance

In this subsection, searching complexity of the proposed scheme is discussed with an example. In addition, the PAPR reduction performance of the proposed scheme is demonstrated by computer simulation. The OFDM system in the simulation employs 128 subcarriers ($N_{\mathrm{C}} = 128$) and QPSK modulation. The codeword length of the IS-LDPC codes is $N = 1024$ and each codeword is transmitted by four OFDM symbols, i.e., $K = 4$. Punctured IS-LDPC codes are employed and the effective code rate is set to $1/2$. The degree distribution pair for the codes is optimized by the density evolution technique [12], with the maximum variable node degree $d_{v_{max}} = 15$. The OFDM signal is four times oversampled to better approximate the PAPR of continuous-time OFDM signals.

The IS-LDPC codes employed in the OFDM system have U disjoint invertible subsets, and the uth invertible subset is $\mathcal{S}_u = \{u, u+U, \cdots, N-U+u\}$ for $u = 1, 2, \cdots, U$. Coded bits of $\mathcal{S}_{(k-1)U/4+1}$ to $\mathcal{S}_{kU/4}$ are randomly mapped onto the subcarriers of the kth OFDM symbol, $k = 1, 2, 3, 4$. By this assignment, the proposed scheme has a manageable searching complexity, due to the fact that the number of invertible subsets in each OFDM symbol is U/K. For example, when $U = 32$, the number of searching is 2^8 for each OFDM symbol, and the number of searching is 4×2^8 for each codeword. In contrast, for the scheme of [17] with a conventional LDPC code and 32 label bits, the number of searching is 2^{32} for each codeword, which is 2^{22} times that of the proposed scheme. This example demonstrates that, the searching complexity of the proposed PAPR scheme is dramatically less than that of [17] for OFDM systems with multiple-OFDM-symbol frames, when K is large.

To demonstrate the PAPR performance of the proposed scheme, PAPR performance of the PTS scheme, which is a typical candidate generation scheme, is presented for comparison. The PTS scheme employs random partition [2] [25] and its phase factors are chosen from $\{+1, -1\}$. Fig. 12 plots the complementary cumulative distribution functions (CCDF) of the PAPRs. It is observed that, the PAPR reduction increases with the number of candidates (2^U), and the proposed scheme offers about 0.7 dB, 2.4 dB, 4.1 dB PAPR reduction at CCDF $= 10^{-4}$, when $U = 8, 16$ and 32, respectively. Note that in this simulation, inverting a bit means the inverting of the in-phase or quadrature component of corresponding QPSK symbol, since the coded bits of all invertible subsets are mapped onto sign bits of symbols. Due to this equivalence, it is not surprising that the proposed PAPR scheme has the similar PAPR performance as the PTS scheme, when U/K (the number of invertible subsets per OFDM symbol) equals to W (the number of PTS partitions). Therefore, the proposed scheme has the similar searching complexity and PAPR reduction performance as the PTS scheme, as long as the candidate number of each OFDM symbol is the same for both schemes.

Based on the above simulation results, we conclude: compared with the existing coding-based candidate generation schemes, the proposed scheme dramatically reduces the searching complexity, when K is large; and the proposed scheme achieves typical PAPR reduction performance of candidate generation schemes.

VIII. Conclusions and Future Works

In this paper, we proposed a novel type of LDPC codes (IS-LDPC code) for PAPR reduction in OFDM systems. The advantages of the proposed IS-LDPC codes could be summarized as follows:

- Compared with the existing coding-based candidate generation schemes, the proposed scheme reduces the searching complexity from 2^U to $K2^{U/K}$, where 2^U is the number of candidates for each codeword and K is the number of OFDM symbols employed to transmit the codeword. Obviously, the reduction of searching complexity is dramatic when K is large.
- The IS-LDPC codes exhibit excellent error performance, which is very close to that of the LDPC codes constructed by the PEG algorithm, for a wide range of U.
- The proposed PAPR reduction scheme demonstrate similar PAPR performance as the PTS scheme, when U/K (the number of invertible subsets per OFDM symbol) equals to W (the number of PTS partitions).

Due to the dramatically reduced searching complexity and excellent error performance, the IS-LDPC codes make it possible to support huge number of candidates for PAPR reduction, which is especially essential for OFDM systems that employs multiple OFDM symbols to transmit a codeword. Therefore, the proposed PAPR reduction scheme based on IS-LDPC codes could serve as an attractive PAPR reduction solution for future multicarrier communication systems.

In the future works, we aim to improve the error performance of IS-LDPC codes with higher inversion freedom, and design more practical IS-LDPC codes, such as quasi-cyclic IS-LDPC codes.

References

[1] S. H. Han and J. H. Lee, "An Overview of Peak-to-Average Power Ratio Reduction Techniques For Multicarrier Transmission," *IEEE Wireless Communications,* vol. 12, no. 2, pp. 56-65, Apr. 2005.

[2] T. Jiang and Y. Wu, "An overview: peak-to-average power ratio reduction techniques for OFDM signals," *IEEE Transactions on Broadcasting,* vol. 54, no. 2, pp. 257-268, Jun. 2008.

[3] A. E. Jones, T. A. Wilkinson, and S. K. Barton, "Block coding scheme for reduction of peak to mean envelope power ratio of multicarrier transmission schemes," *IEE Electronics Letters,* vol. 30, pp. 2098-2099, Dec. 1994.

[4] K. G. Paterson and V. Tarokh, "On the existence and construction of good codes with low peak-to-average power ratios," *IEEE Transactions on Communications,* vol. 46, pp. 1974-1987, Sept. 2000.

[5] V. Tarokh and H. Jafarkhani, "On the computation and reduction of the peak-to-average power ratio in multicarrier communications," *IEEE Transactions on Communications,* vol. 48, no. 1, pp. 37-44, Jan. 2000.

[6] J. A. Davis and J. Jedwab, "Peak-to-mean power control in OFDM, Golay complementary sequences, and Reed-Muller codes," *IEEE Transactions on Information Theory,* vol. 45, no. 7, pp. 2397-2417, Nov. 1999.

[7] K. U. Schmidt, "On cosets of the generalized first-order Reed-Muller code with low PMEPR," *IEEE Transactions on Information Theory,* vol. 52, no. 7, pp. 3220-3232, Jul. 2006.

[8] T. Jiang and G. X. Zhu, "Complement block coding for reduction in peak-to-average power ratio of OFDM signals," *IEEE Communications Magazine,* vol. 43, no. 9, pp. S17-S22, Sept. 2005.

[9] M. Sabbaghian, Y. Kwak, B. Smida, and V. Tarokh, "Near Shannon limit and low peak to average power ratio turbo block coded OFDM," *IEEE Transactions on Communications,* vol. 59, no. 8, pp. 2042-2045, Aug. 2011.

[10] M. Sabbaghian, Y. Kwak, and V. Tarokh, "New codes from dual BCH codes with applications in low PAPR OFDM," *IEEE Transactions on Wireless Communications,* vol. 10, no. 12, pp. 3990-3994, Dec. 2011.

[11] R. G. Gallager, "Low density parity check codes," *IRE Transactions on Information Theory,* vol. IT-8, pp. 21-28, Jan. 1962.

[12] T. J. Richardson, A. Shokrollahi, and R. Urbanke, "Design of capacity approaching irregular low-density parity-check codes," *IEEE Transactions on Information Theory,* vol. 47, no. 2, pp. 619-637, Feb. 2001.

[13] X. Y. Hu, E. Eleftheriou, and D. M. Arnold, "Regular and irregular progressive edge-growth Tanner graphs," *IEEE Transactions on Information Theory,* vol. 51, no. 1, pp. 386-398, Jan. 2005.

[14] M. P. C. Fossorier, "Quasi-cyclic low-density parity-check codes from circulant permutation matrices," *IEEE Transactions on Information Theory,* vol. 50, no. 8, pp. 1788-1793, Aug. 2004.

[15] L. Zhang, Q. Huang, S. Lin, K. A. Ghaffar and I. Blake, "Quasi-cyclic LDPC codes: an algebraic construction, rank analysis, and codes on Latin squares", *IEEE Transactions on Communications,* vol. 58, no. 11, pp. 3126-3139, Nov. 2010.

[16] Q. Huang, S. Lin and K. Abdel-Ghaffar, "Cyclic and quasi-cyclic LDPC codes on constrained parity-check matrices and their trapping sets," *IEEE Transactions on Information Theory,* vol. 58, no. 5, pp. 2648-2671, May 2012.

[17] H. Breiling, S. H. Muller-Weinfurtner, and J. B. Huber, "SLM Peak-Power reduction without explicit side information," *IEEE Communications Letters,* vol. 5, no. 6, pp. 239-241, Jun. 2001.

[18] Y. C. Tsai, S. K. Deng, K. C. Chen, M. C. Lin, "Turbo coded OFDM for reducing PAPR and error rates," *IEEE Transactions on Wireless Communications,* vol. 7, no. 1, pp. 84-89, Jan. 2008.

[19] Y. Xin and I. J. Fair, "Error-control selective mapping coding for PAPR reduction in OFDM systems," *Proc. IEEE 60th Vehicular Technology Conference,* pp. 583-587, Sept. 2004.

[20] G. S. Yue and X. D. Wang, "A hybrid PAPR reduction scheme for coded OFDM," *IEEE Transactions On Wireless Communications,* vol. 5, no. 10, pp. 2712-2722, Oct. 2006.

[21] H. Chen and H. Liang, "PAPR reduction of OFDM signals using partial transmit sequences and Reed-Muller codes," *IEEE Communications Letters,* vol. 11, no. 6, pp. 528-530, Jun. 2007.

[22] H. Chen and H. Liang, "Combined Selective Mapping and Binary Cyclic Codes for PAPR Reduction in OFDM Systems," *IEEE Transactions on Wireless Communications,* vol. 6, no. 10, pp. 3524-3539, Oct. 2007.

[23] R. Fischer, C. Siegl, "Reed Solomon and simplex codes for peak to average power ratio reduction in OFDM," *IEEE Transactions on Information Theory,* vol. 55, no. 4, pp. 1519-1528, Apr. 2009.

[24] R. W. Bauml, R. F. H. Fisher, and J. B. Huber, "Reducing the peak-to-average power ratio of multicarrier modulation by selected mapping," *IEE Electronics Letters,* vol. 32, no. 22, pp. 2056-2057, Oct. 1996.

[25] S. H. Muller and J. B. Huber, "OFDM with reduced peak-to-average power ratio by optimum combination of partial transmit sequences," *IEE Electronics Letters,* vol. 33, no. 5, pp. 36-69, Feb. 1997.

[26] A. D. S. Jayalath and C. Tellambura, "SLM and PTS peak-power reduction of OFDM signals without side information," *IEEE Transactions on Wireless Communications,* vol. 4, no. 5, pp. 2006-2013, Sept. 2005.

[27] O. Muta and Y. Akaiwa, "Weighting factor estimation method for peak power reduction based on adaptive flipping of parity bits in Turbo-coded OFDM systems," *IEEE Transactions on Vehicular Technology,* vol. 57, no. 6, pp. 3551-3562, Nov. 2008.

[28] L. Li and D. Qu, "Joint Decoding of LDPC Code and Phase Factors for OFDM Systems With PTS PAPR Reduction," to appear in *IEEE Transactions on Vehicular Technology*.

[29] S. Y. Le Goff, S. S. Al-Samahi, B. K. Khoo, C. Tsimenidis, and B. S. Sharif. "Selected mapping without side information for PAPR reduction in OFDM," *IEEE Trans. on Wireless Comms.,* vol. 8, no. 7, July 2009, pp. 3320-3325.

[30] W. S. Ho, A. S. Madhukumar, and F. Chin, "Peak-to-average power reduction using partial transmit sequences: A suboptimal approach based on dual layered phase sequencing," *IEEE Transactions on Broadcasting,* vol. 49, no. 2, pp. 225-231, Jun. 2003.

[31] S. H. Han and J. H. Lee, "PAPR reduction of OFDM signals using a reduced complexity PTS technique," *IEEE Signal Processing Letters,* vol. 11, no. 11, pp. 887-890, Nov. 2004.

[32] T. Jiang, W. D. Xiang, P. C. Richardson, J. H. Guo, and G. X. Zhu, "PAPR reduction of OFDM signals using partial transmit sequences with low computational complexity," *IEEE Transactions on Broadcasting,* vol. 53, no. 3, pp. 719-724, Sept. 2007.

[33] A. Ghassemi and T. A. Gulliver, "PAPR reduction of OFDM using PTS and error-correcting code subblocking," *IEEE Transactions On Wireless Communications,* vol. 9, No. 3, pp. 980-989, Mar. 2010.

[34] IEEE Std 802.11a/D7.0 1999, *Part 11: Wireless LAN Medium Access Control (MAC) and Physical Layer (PHY) specifications: High Speed Physical Layer in the 5GHz Band.*

[35] T. Tian, C. Jones, J. D. Villasenor, and R. D. Wesel, "Selective avoidance of cycles in irregular LDPC code construction," *IEEE Transactions on Communications,* vol. 52, no. 8, pp. 1242-1248, Aug. 2004.

[36] H. Xiao and A. H. Banihashemi, "Improved progressive-edge-growth (PEG) construction of irregular LDPC codes," *IEEE Communications Letters,* vol. 8, no. 12, pp. 715-717, Dec. 2004.

[37] D. Vukobratovic and V. Senk, "Generalized ACE constrained progressive edge growth LDPC code design," *IEEE Communications Letters,* vol. 12, no.1, pp. 32-34, Jan. 2008.

[38] D. Vukobratovic and V. Senk, "Evaluation and design of irregular LDPC codes using ACE spectrum," *IEEE Transactions on Communications,* vol. 57, no. 8, pp. 2272-2278, Aug. 2009.

[39] J. Hou, P. H. Siegel, and L. B. Milstein, "Performance analysis and code optimization of low density parity-check codes on Rayleigh fading channels," *IEEE Journal Selected Areas on Communications,* vol. 19, no. 5, pp. 924-934, May. 2001.

[40] M. Luby, M. Mitzenmacher, A. Shokrollahi, and D. Spielman, "Improved low-density parity-check codes using irregular graphs," *IEEE Transactions on Information Theory,* vol. 47, pp. 585-598, Feb. 2001.